Supporting Information

Interminiband optical transitions in graphene lateral superlattices

Yuyu Li and Roberto Paiella

Department of Electrical and Computer Engineering and Photonics Center,

Boston University, 8 Saint Mary's Street, Boston, MA 02215

S1. Interminiband absorption versus scattering lifetime

Figure S1 shows the interminiband absorption spectrum of the same superlattice (SL) of Fig. 2 of the main text (having period Λ = 50 nm and potential U_{SL} = 73 meV), computed for different values of the carrier scattering lifetime τ_{sc}. In these calculations, the sample is taken to be in thermal equilibrium at 5 K, with Fermi energy E_F aligned to the top of the third valence miniband V3. For all values of τ_{sc} considered in the figure (ranging from 1 ps to 200 fs), a pronounced absorption peak centered near 3.7 THz is observed, which is once again due to electronic transitions near the X point of the mini-Brillouin zone (MBZ) between minibands V3 and V2. As the scattering lifetime is decreased, the absorption peak decreases and broadens as expected. However, it remains quite strong across the entire range of values of τ_{sc} considered in the figure. In particular, even for τ_{sc} = 200 fs the peak absorption coefficient is found to be as large as about 2.2, corresponding to a single-pass absorbance through the graphene layer $1 - e^{-\alpha} = 88.9$ %.

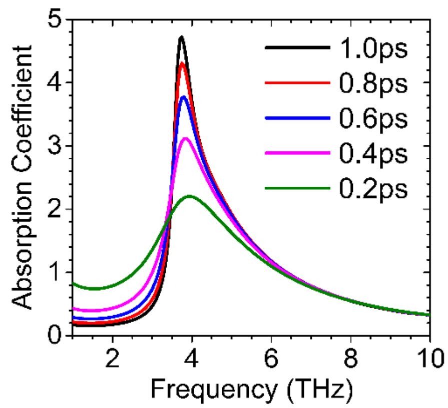

Figure S1. Interminiband absorption spectrum of the same SL of Fig. 2 of the main text (at a temperature of 5 K), for different values of the scattering lifetime τ_{sc}.

S2. Interminiband absorption versus superlattice period

Figure S2 illustrates how interminiband absorption in the structures under study depends on the SL period Λ. The color map of Fig. S2(a) shows the low-temperature absorption spectrum of a device with Λ = 30 nm for different values of the SL potential U_{SL}. The observed dependence on U_{SL} is similar to the behavior displayed in Fig. 3(a) of the main text (for a 50-nm-period device), except for a significantly larger tuning range of the frequency of peak absorption ν_{peak}. The underlying reason is the increase in the size of the MBZ (and therefore in the energy dispersion of minibands V2 and V3 within the MBZ) with decreasing SL period. As a result, the flattening of both minibands with increasing SL potential, which is responsible for the observed saturation in ν_{peak}, occurs at higher values of U_{SL} in SLs of shorter period. This conclusion is confirmed by the simulation results shown in Fig. S2(b), where ν_{peak} is plotted as a function of U_{SL} for five different SLs of different period Λ.

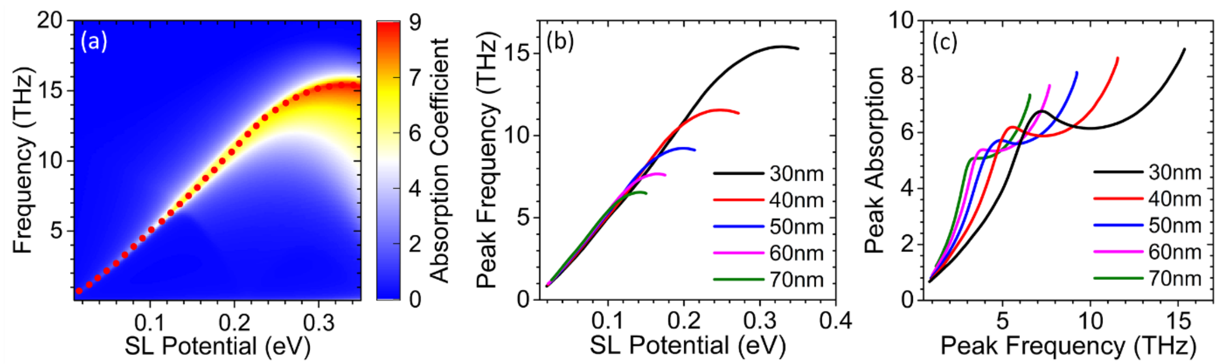

Figure S2. (a) Interminiband absorption spectrum of a SL based on the geometry of Fig. 1(a) of the main text with period Λ = 30 nm, for different values of the SL potential U_{SL}. (b) Frequency of peak absorption ν_{peak} plotted as a function of U_{SL} for different values of Λ. In all these simulations, the SL is taken to be in thermal equilibrium at 5 K, with Fermi level aligned to the top of miniband V3. (c) Peak absorption coefficient α_{peak} versus ν_{peak} for different values of Λ.

As illustrated in Fig. S2(a) and Fig. 3(a) of the main text, varying the SL potential has the effect of changing both the frequency of peak absorption ν_{peak} and the peak absorption coefficients α_{peak}. In Fig. S2(c), the resulting dependence of α_{peak} on ν_{peak} is plotted for the five different periods considered in Fig. S2(b). It follows from these results that longer-period SLs are preferable for operation at lower frequencies, where they can provide larger interminiband absorption. In contrast, higher frequencies can only be accessed with proportionally shorter periods.

S3. Pump-wavelength optimization

The pump wavelength λ_p used in the gain calculations presented in the main text is selected so as to maximize r_3 while at the same time keeping r_2 as small as possible, where the generation rate r_n (for n = 2 or 3) is the fraction of incident pump photons that are absorbed through the creation of holes in miniband Vn. This selection of λ_p is favorable to maximize the interminiband gain coefficient under study, which increases with increasing hole density in V3 and with decreasing hole density in V2. The parameters r_n are computed as follows

$$r_n = \frac{\alpha_{\mathrm{V}n}}{\alpha_{\mathrm{tot}}}(1 - e^{-\alpha_{\mathrm{tot}}}), \tag{S1}$$

where α_{tot} is the total absorption coefficient and $\alpha_{\mathrm{V}n}$ is the contribution involving only electronic transitions out of miniband Vn. In eq. (S1), the quantity in parentheses is the total fraction of incident pump photons (transmitted inside the graphene sheet) that are absorbed by the SL, and the ratio $\alpha_{\mathrm{V}n}/\alpha_{\mathrm{tot}}$ accounts for the portion of such photons that produce holes in miniband Vn. The absorption coefficients α_{tot} and $\alpha_{\mathrm{V}n}$ are computed using eq. (1) of the main text, including all possible transitions involving at least the eight lowest conduction and valence minibands.

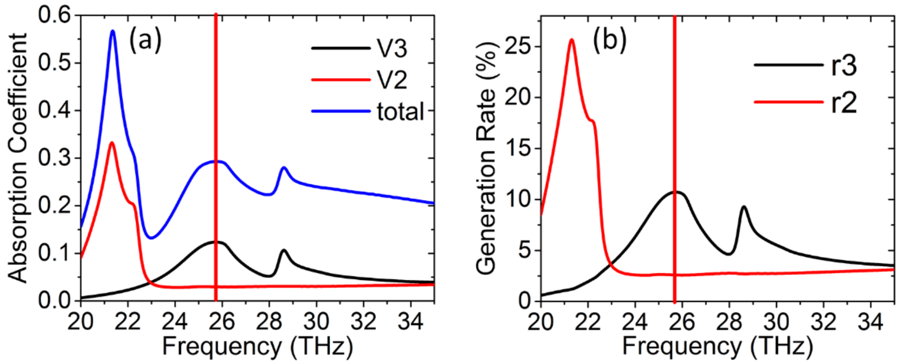

Figure S3. (a) Absorption spectra α_{tot}, α_{V3}, and α_{V2} of an undoped SL based on the geometry of Fig. 1(a) of the main text with Λ = 50 nm and U_{SL} = 73 meV at 5 K. (b) Generation rates r_3 and r_2 computed from the absorption spectra of (a) using eq. (S1). The vertical lines in (a) and (b) indicate the pump frequency $\nu_p = c/\lambda_p$ selected for the gain calculations based on these simulation results.

In Fig. S3(a), α_{tot}, α_{V3}, and α_{V2} are plotted as a function of optical frequency ν for a 50-nm-period undoped SL (i.e., with Fermi energy $E_{\mathrm{F}} = 0$) at 5 K under the bias conditions of Fig. 1 (U_{SL} = 73 meV). The corresponding generation rates r_3 and r_2 are shown in Fig. S3(b). Based on these data, we select a pump wavelength λ_p of 11.7 μm, corresponding to the optical frequency $\nu_p = c/\lambda_p$ shown by the vertical line in Figs. S3(a) and S3(b). The peak in α_{V3} (and therefore in r_3) at this frequency originates from electronic transitions between minibands V3 and C1 involving states near the Γ-X and Γ-M symmetry lines, where the two minibands feature very similar slopes [see Fig. 1(c) of the main text]. Since the miniband structure depends on the SL potential, the procedure just described has been repeated for all values of U_{SL} considered in the main text. The resulting optimal values of λ_p vary within the relatively small range of 11.7 to 12.4 μm.

S4. Interminiband gain versus temperature

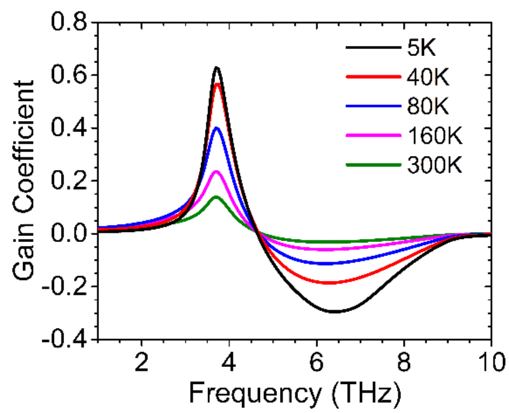

Figure S4. Interminiband gain spectrum of the same SL of Fig. 4 of the main text (for an interminiband relaxation lifetime τ* of 3 ps), at different temperatures.

Figure S4 shows the interminiband gain spectrum of a 50-nm-period undoped SL at different temperatures, computed with the same model used in Fig. 4 of the main text and assuming an interminiband relaxation lifetime τ* of 3 ps. In these calculations, the SL potential is U_{SL} = 73 meV, and the incident pump light has wavelength λ_p = 11.7 μm and intensity (transmitted inside the graphene sheet) equivalent to 5 mW focused on a 10×10 μm^2 area. A relatively small but still experimentally accessible peak gain coefficient g = 0.14 is obtained at room temperature, corresponding to an intracavity amplification factor per round trip e^{2g} of 1.3×. In any case, it should be emphasized that a more definitive determination of the temperature dependence of these gain spectra requires a more detailed knowledge of the intra- and interminiband relaxation dynamics of graphene SLs than presently available.